



Voltammetric pH Sensor based on an Edge Plane Pyrolytic Graphite Electrode

Journal:	<i>Analyst</i>
Manuscript ID:	AN-ART-01-2014-000147.R1
Article Type:	Paper
Date Submitted by the Author:	10-Mar-2014
Complete List of Authors:	Lu, Min; Oxford University, Compton, Richard; Oxford University, Department of Chemistry

Voltammetric pH Sensor based on an Edge Plane Pyrolytic Graphite Electrode

Authors: Min Lu, Richard G. Compton*

*Corresponding author

Department of Chemistry, Physical and Theoretical Chemistry Laboratory, Oxford University, South Parks Road, Oxford, United Kingdom, OX1 3QZ

Submitted to : The Analyst

Abstract

A simple sensor for pH determination is reported using *unmodified* edge plane pyrolytic graphite (EPPG) electrodes. The analysis is based on the electro-reduction of surface quinone groups on the EPPG which was characterised using cyclic voltammetry (CV) and optimised with square-wave voltammetry (SWV). Under optimised conditions, a linear response is observed between the peak potential and pH with a gradient of ~ 59 mV per pH (at 25°C), which corresponds well with Nernstian behaviour based on a 2 proton, 2 electron system over the aqueous pH range 1.0 to 13.0. As such, an EPPG is suggested as a reagent free and robust pH sensing materials.

Introduction

The determination of pH is fundamental to the study of chemical and biochemical reactions in aqueous solution, with measurements carried out extensively in both industrial and academic environments¹. Its widespread application includes uses in the food industry, agriculture, the biopharmaceutical industry, medicine and water treatment²⁻⁴.

pH sensors are mainly potentiometric or amperometric^{5, 6}, however methods for pH determination also include using fluorescent agents^{7, 8}, NMR methods⁹ amongst many others¹⁰. At present, the use of glass electrodes¹¹ is the most common potentiometric approach due to their high sensitivity and selectivity, reasonably fast response, availability from commercial sources, and if carefully handled, long lifetimes. They are, however, fragile due to their glass nature and can be impractical to use for “in-field” analysis. In addition, glass electrodes can suffer from instability and potential drift¹² as a result of decreased sensitivity towards hydrogen activity caused by dehydration of the glass membrane¹³. They also suffer from “alkali errors”¹⁴. This approach requires regular and

1
2
3 frequent re-calibration prior to use. Amperometric pH sensors utilising polymer films^{15, 16}, enzymes
4¹⁷ and organic redox species¹³ have been explored to address the various drawbacks related to
5
6 potentiometric sensing.
7

8
9 Amperometric electrochemical pH sensors featuring polymer films or chemical modification
10 of the electrode often involve attaching quinone functionality onto the surface¹⁸. Tarasevich et al.¹⁹
11 observed redox processes related to quinoid group reactions, and further investigations revealed the
12 effect of pH on these redox processes. The voltammetric response can be quantified using the
13 Nernst equation²⁰,
14
15

$$E_p = E_{formal}^{\circ} - \frac{2.3 RTm}{nF} pH$$

16
17
18
19
20 where m , n = number of protons and electrons involved in the redox process, respectively. There is
21 thus a correlation between the peak potential and pH for the reduction of quinones. In particular,
22 for $n = 2$, slopes of ca. 0, 30 and 60 mV per pH unit are seen for $m = 0, 1$ and 2. The response of the
23 quinone reduction has been reviewed by Guin et al.²¹ and forms the basis of many modified pH
24 sensors. A schematic showing three possible reduction pathways of an ortho-benzoquinone, along
25 with associated protonations is given in Figure 1 where $n = 2$ and $m = 0, 1, 2$. Literature pK_a values
26 for ortho-benzoquinone are pK_{a1} 9.25 and pK_{a2} 13.0 in aqueous solution at 25°C²². Quinones and
27 their electrochemical properties have been extensively studied previously, and the $2H^+/2e^-$ “scheme
28 of squares” model²³ has been proposed assuming that electron transfer is the rate limiting step and
29 the H^+ are at equilibrium in well buffered media²⁴.
30
31
32
33
34
35
36
37

38 Carbon is a highly attractive material, commonly employed in electrochemistry and widely
39 used as an electrode material²⁵⁻²⁷. This can be attributed to its good conductivity, ready availability,
40 versatility, wide working potential range and low cost. The surface chemistry of carbon is highly
41 complex, extensive, and often decorated with many functional groups which sometimes can react
42 easily with other molecules^{28, 29}. A representation of various functional groups present on graphitic
43 carbon surfaces is shown in Figure 2²⁹.
44
45
46
47

48 Characterisation of the carbon surface has been studied by many researchers to identify
49 surface oxo-groups^{28, 30, 31}. In the case of edge plane pyrolytic graphite (EPPG) electrode, the defect
50 sites present on the carbon surface can easily react with oxygen in the atmosphere to form a variety
51 of oxo-groups on the surface, including quinonyl, carbonyl and hydroxyl functional groups²⁸ and
52 these are suggested sites for electron transfer processes³².
53
54
55
56
57
58
59
60

1
2
3 Carbon materials with surface modification and derivatization have been developed for
4 reliable pH determination; Kahlert comprehensively summarises many of these methods ¹. Some
5 patents have also been filed using *functionalized* carbon electrodes as a basis for electrochemical pH
6 sensors ³³⁻³⁶.
7
8
9

10 In this paper, in contrast and novelly, we exploit the *intrinsic* presence of quinone groups
11 available on EPPG surfaces and use cyclic voltammetry (CV) and square wave voltammetry (SWV) to
12 study the effect of pH on the reduction of the surface quinones. It is surprising and somewhat
13 unexpected, but very useful that a linear response was observed over the entire pH range. Given
14 that the pK_a of ortho-benzoquinone is 9.25 in solution, one would expect a gradient consistent for m
15 = 2 to be limited to ca. pH 9.0 and below; however we report a linear pH dependent response up to
16 pH 13.0 at an EPPG electrode. The observed shift in reduction peak potential is in good agreement
17 with the theoretically predicted value of ca. 58 mV per pH for T = 298 K, for a Nernstian manner,
18 suggesting the feasibility for the EPPG electrode to work as a pH sensor over the full pH range 1.0 to
19 13.0. Note that previous studies ³⁷⁻³⁹ have shown that very significant shifts for pK_a are possible for
20 molecules tethered to carbon electrode surfaces and so in this light, the observed behaviour may be
21 rationalised.
22
23
24
25
26
27
28
29
30
31
32
33
34

35 Experimental

36 (a) Apparatus

37
38
39 All voltammetric measurements were recorded using a μ -Autolab-II computer controlled
40 potentiostat (Metrohm-Autolab BV), and operated by GPES software. A standard three-electrode
41 configuration consisting of a saturated calomel reference electrode (SCE) (Hach Lange, UK), a
42 platinum (Pt) mesh counter electrode and an edge plane pyrolytic graphite (EPPG) working electrode
43 was used throughout. The EPPG electrode was made from pieces of highly ordered pyrolytic
44 graphite (HOPG) (Le Carbone Ltd., Sussex, U.K.) of SP13 (ZYH) grade, and machined to discs 4.9 mm
45 in diameter and 0.5 mm in length. By orientating the disc face perpendicular to the graphite crystal
46 surface, an edge plane was achieved; these were then set in custom made PTFE housing with an
47 electrical connection made using a stainless steel core.
48
49
50
51
52
53
54

55 All pH measurements were conducted using a pH213 Microprocessor pH meter (Hanna
56 instruments, UK). Prior to the measurement of solutions, the pH meter was calibrated using Duracal
57
58
59
60

1
2
3 buffers of pH 4.01 ± 0.01 , pH 7.00 ± 0.01 and pH 10.01 ± 0.01 (Hamilton, CH). Using a 2 point
4 calibration, the manufacturer's specifications state a working range of pH -2.0 to 16.0.
5
6

7 All experiments were performed within a thermostatted Faraday cage (made in-house), to
8 maintain a constant working temperature of 298 K. Temperature of the solutions were maintained
9 at 298 ± 2 K throughout by placing the solutions within the Faraday cage for two hours to ensure
10 thermal equilibrium. A constant temperature of 298 K was used to ensure that the reduction
11 potential of the peaks do not shift with temperature. A thermometer was used for measurement of
12 the solution during the experiment.
13
14
15
16
17
18
19

20 (b) Reagents and solutions

21

22 All chemicals used were of analytical grade and were used as received without further
23 purification. Solutions were prepared with deionized water and had resistivity no less than 18.2
24 M Ω .cm at 25°C (Millipore, UHQ, Vivendi, UK).
25
26
27

28 The buffer solutions were prepared using HCl/ KCl for the pH range 0.0 – 2.5, citric acid/
29 sodium citrate for the pH range 2.5 – 5.0, monosodium phosphate/ disodium phosphate for the pH
30 range 5.0 – 9.0, sodium carbonate/ bicarbonate for the pH range 9.0 – 11.0, and sodium hydroxide
31 for the pH range 12.0 – 13.0. All solutions were made with supporting electrolyte of 100 mM KCl
32 added to each solution. Measurement of the pH was carried out on each freshly made solution prior
33 to experiments.
34
35
36
37

38 All measurements were carried out in a degassed system where solutions were purged with
39 pure N₂ gas (BOC, Guildford UK) prior to experiments for a minimum of 20 minutes in a seal tight
40 environment.
41
42
43
44
45

46 (c) Experimental procedure

47

48 A range of buffer solutions were prepared and their pH determined using a pH meter prior
49 to experiments. A small volume of each solution was taken and transferred into an electrochemical
50 cell where a degassed system was established through thorough bubbling of pure N₂ into the vessel
51 to remove dissolved oxygen in solution. The platinum mesh counter electrode was flamed before
52 the experiment to ensure a clean set-up. The system was thermostatted to maintain temperature at
53 295 ± 2 K.
54
55
56
57
58
59
60

1
2
3 The surface of the EPPG electrodes were thoroughly polished using alumina slurry (Buehler
4 Ltd) on soft lapping pads of decreasing grades, from 1.0 μm to 0.3 μm and finally 0.01 μm , followed
5 by sonication and thorough rinsing using Millipore water. With the EPPG electrode acting as working
6 electrode, cyclic voltammograms were performed to observe the redox properties of the surface
7 quinones. However, optimised results were achieved by observing reductive cathodic scans with
8 square wave voltammetry to more precisely determine the location of the peak potential. The
9 optimised parameters for SWV were: frequency – 150 Hz, step potential – 2 mV, amplitude – 200
10 mV, over the entire pH range explored. The EPPG was used to scan in the cathodic direction, with
11 the potential window adjusted for different pHs to best observe the reduction peak.
12
13
14
15
16
17
18
19
20
21

22 Results and discussions

23
24 Initially, a cyclic voltammogram (CV) was recorded of the bare EPPG surface; a typical CV signal
25 performed in 0.01 M HNO_3 with 100 mM KCl supporting electrolyte can be seen in Figure 3, with the
26 peak potential of the quinone reduction occurring at 221 mV vs. SCE. From this, the surface coverage
27 can be deduced by using the peak area of the reduction peak to determine the quinone surface
28 coverage, according to $Q = nFA\Gamma$, where Γ represents the surface coverage, n represents the number
29 of electrons transferred per molecule, F is the Faraday constant and A is the electrode area. The
30 average value for the surface coverage of quinones was calculated to be $5.9 \times 10^{-11} \pm 0.6 \times 10^{-11}$ mol
31 cm^{-2} , with $n = 2$. After establishing optimised parameters for the cathodic scans of the surface
32 quinone reduction in square wave, all analyses were performed on the respective square wave
33 voltammetric results.
34
35
36
37
38
39
40

41 Using a range of 0.01 M pH buffer solutions, a single peak was observed by scanning
42 cathodically from positive to negative potentials in square wave voltammetry as shown in Figure 4.
43 Since the pH for the 0.01 M HCl/KCl buffer solution was pH2.11, a 0.1 M HCl/KCl buffer solution was
44 investigated and included for completeness to observe the response between the peak potential and
45 full pH range. The pH of the 0.1M HCl/KCl buffer in this case was 1.09. Three sets of reductions were
46 performed which corresponds to solutions in the low (0.0 – 5.0), neutral (5.0 – 9.0) and high (9.0 –
47 14.0) pH range using HCl/ KCl and citrate buffer solutions, monosodium phosphate/ disodium
48 phosphate buffer solutions and sodium carbonate/ bicarbonate and sodium hydroxide solutions,
49 respectively. Using HCl/ KCl and citrate buffers, as in Figure 4(a), the reduction peak potential shifts
50 from 222 mV at pH 2.11 to 71 mV at pH 4.93. Similarly, for other buffers shown in Fig 4 (b) and (c),
51 an increase in pH from 5.62 to 8.38 resulted in a peak potential shift from 1 mV to -172 mV, and for
52
53
54
55
56
57
58
59
60

1
2
3 pH 9.39 to 12.9, the reduction peak potential changes from -207 mV to -402 mV, respectively. The
4 potential window was increased for higher pH solutions to accommodate for the shift in potential
5 with pH. A composite of all the reductions peaks in different buffer solutions can be seen in Figure 5.
6 It can be observed that by increasing pH, peak potentials shift in the cathodic direction towards
7 more negative values. At high pH, there are fewer protons available for the $2\text{H}^+/2\text{e}^-$ reduction
8 process, and as a result, probably limits the extent of quinone reduction resulting in less well
9 resolved signals and lower currents. Background correction and smoothing of the signals allowed
10 enhancement of the peaks for analysis. Both methods were performed using GPES software; the
11 background correction involved subtracting a 2nd order polynomial baseline curve from the raw data,
12 whilst background noise was smoothed using the Savitzky and Golay smoothing filter^{40, 41}.

13
14
15
16
17
18
19
20 Polishing of the EPPG electrode for 20 minutes prior to each experiment exposed surface
21 quinone functional groups, which were used to explore the electrode response to varying pH. By
22 measuring the peak potential of the reduction peaks in SWV and plotting against pH, a linear
23 response could be seen in the pH 1.0 – 13.0 range, as shown in Figure 6. The gradient of the slope
24 was 57.0 ± 1.0 mV per pH which is consistent with a linear Nernstian response corresponding to a
25 two-electron, two-proton electrochemical process where m , n = number of protons and electrons
26 involved in the redox process, respectively, $T = 298$ K. The linear slope produced from the peak
27 potential vs. pH graph highlights the pH sensitive nature of the quinone groups on the surface of the
28 EPPG electrode. By examining the pK_a values for ortho-benzoquinone in aqueous solution, pK_{a1} 9.25
29 and pK_{a2} 13 (Figure 1), we can infer significant differences in pK_a must exist between such molecules
30 in bulk solution and similar structures present at the surface. If the surface quinones showed similar
31 pK_a values to those displayed in solution, one would expect changes in gradient at high pH around
32 pH 9.0 and 13.0. However, the gradient consistent for $m = 2$ was observed for the full aqueous pH
33 1.0 – 13.0 range. It can be assumed that deprotonation of the surface hydro-orthoquinone
34 molecules does not occur below ca. pH 13, and so extensive pH measurements can be carried out
35 even at high pH without the need for modification of the electrode to achieve a linear Nernstian
36 response. We note that significant changes in pK_a have been reported for molecules immobilised on
37 electrode surfaces^{37-39, 42}.

38
39
40
41
42
43
44
45
46
47
48
49
50 The mechanism of the quinone reduction in neutral solutions, involving a 2 proton / 2
51 electron process, can lead to charged intermediates being possibly formed. At neutral pHs, this can
52 be a semi-quinone species. Stabilization of semiquinone intermediates have been proposed in the
53 literature^{42, 43}.

1
2
3 To explore the possibilities of semi-quinones contributing to the SWV signal, the SWV
4 parameters were altered, and the amplitude lowered from 200 mV to 20 mV. It was observed that
5 phosphate buffers within the pH range 5.0 – 9.0 produced a double peak or splitting of the peak.
6 Their reduction in SWV with amplitude 20 mV can be seen Figure 7(a) whilst the overcompensated
7 scans at 200 mV amplitude can be seen in Figure 7(b). Lowered amplitude parameters with buffers
8 outside of the neutral pH range were also investigated, but produced just one single peak, which
9 suggests that the semiquinone intermediate is stabilised observed only in environments around pH
10 7.
11
12
13
14
15

16
17 The reduction potential of the double peaks shown in Figure 7(a) were plotted in Figure 8,
18 together with the reduction peaks obtained with amplitude 200mV. The red circles and black
19 squares represent the two positions of the double peak reduction, whilst the blue triangles
20 correspond to the peaks with amplitude 200 mV. It can be seen that the position of the reduction
21 peaks at the higher amplitude is intermediate between the split peak values.
22
23
24
25
26
27
28
29

30 Investigating the effects of changing ionic strength and buffer concentration

31
32
33 Having calibrated successfully for the 0.01 M buffer solutions, further investigation into
34 higher concentration solutions were performed to see the effects of increasing ionic strength.
35
36

37 0.1 M citrate, phosphate and carbonate buffer solutions all produced a single reduction peak
38 as seen in Figure 9. Taking the reduction peak potential and plotting against pH, as in Figure 10, the
39 calibration gives a linear response with a gradient of 59.0 mV/ pH. By plotting these points against
40 the original calibration plot across the entire pH range, we can see from Figure 11 that the results
41 (shown as blue triangles) fits well onto the previous results, given as black squares. A line of best fit
42 going through both the 0.01 M and 0.1 M results with a gradient of 58 mV/ pH could be produced
43 using the parameters as specified earlier.
44
45
46
47
48

49 It can be concluded that an EPPG electrode can be used as a pH sensor over the aqueous
50 range 1.0 – 13.0 in solutions of variable ionic strength. Taking the reduction potential of the EPPG in
51 SWV gave reduction peaks which can be easily analysed. Quantitative analysis of the reduction peak
52 potential can thus be used to produce a linear reduction peak potential against pH calibration plot.
53
54
55
56
57
58
59
60

1
2
3 Conclusions
4

5 For an unmodified edge plane pyrolytic graphite electrode (EPPG), the SWV peak potential
6 for the reduction of surface quinones has been shown to respond linearly with solutions of different
7 pH such that a calibration plot ranging from pH 1.0 – 13.0 can be successfully formed. A Nernstian
8 response corresponding to a 2 proton/ 2 electron system lends itself to the use of an EPPG as a
9 simple, easy to use, reagentless and cheap pH sensing material.
10
11
12
13
14
15
16
17
18
19
20
21
22
23
24
25
26
27
28
29
30
31
32
33
34
35
36
37
38
39
40
41
42
43
44
45
46
47
48
49
50
51
52
53
54
55
56
57
58
59
60

1
2
3 References
4
5

- 6 1 H. Kahlert, *J. Solid State Electrochem.*, 2008, **12**, 1255-1266 (DOI:10.1007/s10008-008-0566-7).
7
8 2 V. G. H. Lafitte, W. Wang, A. S. Yashina and N. S. Lawrence, *Electrochem. Commun.*, 2008, **10**, 1831-
9 1834 (DOI:10.1016/j.elecom.2008.09.031).
10
11 3 J. S. Bradley, J. O. Phillips, J. E. Cavanaugh and M. H. Metzler, *Crit Care Med*, 1998, **26**, 1905-1909.
12
13 4 C. Guyard, *Eau, Ind., Nuisances*, 2011, **347**, 87-88, 90, 92, 94-96.
14
15 5 D. R. Turner, M. Whitfield and A. G. Dickson, *Geochim. Cosmochim. Acta*, 1981, **45**, 855-881
16 (DOI:10.1016/0016-7037(81)90115-0).
17
18 6 A. P. F. Turner, I. Karube and G. S. Wilson, *Biosensors: Fundamentals and Applications*, Oxford
19 University Press, Oxford, 1987.
20
21 7 B. K. Kanungo, M. Baral, R. K. Bera and S. K. Sahoo, *Monatsh. Chem.*, 2010, **141**, 157-168
22 (DOI:10.1007/s00706-009-0235-2).
23
24 8 M. Kneen, J. Farinas, Y. Li and A. S. Verkman, *Biophys. J.*, 1998, **74**, 1591-1599 (DOI:10.1016/S0006-
25 3495(98)77870-1).
26
27 9 R. B. Moon and J. H. Richards, *J. Biol. Chem.*, 1973, **248**, 7276-7278.
28
29 10 S. Nomura, *Bunseki*, 2011, **8**, 468-475.
30
31 11 F. G. K. Baucke, *J. Non-Cryst. Solids*, 1985, **73**, 215-231 (DOI:10.1016/0022-3093(85)90348-5).
32
33 12 H. B. Kristensen, A. Salomon and G. Kokholm, *Anal. Chem.*, 1991, **63**, 885A-891A
34 (DOI:10.1021/ac00018a722).
35
36 13 L. Xiong, C. Batchelor-McAuley and R. G. Compton, *Sens. Actuators, B*, 2011, **159**, 251-255
37 (DOI:10.1016/j.snb.2011.06.082).
38
39 14 D. A. Skoog, D. M. West, J. Holler and S. R. Crouch, *Fundamentals of Electro-Analytical Chemistry*,
40 2004.
41
42 15 G. Cui, J. S. Lee, S. J. Kim, H. Nam, G. S. Cha and H. D. Kim, *Analyst (Cambridge, U. K.)*, 1998, **123**,
43 1855-1859 (DOI:10.1039/a802872i).
44
45 16 G. Cheek, C. P. Wales and R. J. Nowak, *Anal. Chem.*, 1983, **55**, 380-381
46 (DOI:10.1021/ac00253a047).
47
48 17 R. M. Greenway, S. J. Gardiner, A. L. Hart and J. Dunlop, *Biosens. Bioelectron.*, 1994, **9**, 457-461
49 (DOI:10.1016/0956-5663(94)90034-5).
50
51 18 G. G. Wildgoose, M. Pandurangappa, N. S. Lawrence, L. Jiang, T. G. J. Jones and R. G. Compton,
52 *Talanta*, 2003, **60**, 887-893 (DOI:10.1016/S0039-9140(03)00150-4).
53
54
55
56
57
58
59
60

- 1
2
3 19 M. R. Tarasevich, V. A. Bogdanovskaya and N. M. Zagudaeva, *J. Electroanal. Chem. Interfacial*
4 *Electrochem.*, 1987, **223**, 161-169 (DOI:10.1016/0022-0728(87)85257-9).
5
6 20 R. G. Compton and C. E. Banks, *Understanding Voltammetry*, Imperial College Press, London,
7 2011.
8
9 21 P. S. Guin, S. Das and P. C. Mandal, *Int. J. Electrochem.*, 2011, , 816202, 22
10 (DOI:10.4061/2011/816202).
11
12 22 N. Schweigert, A. J. B. Zehnder and R. I. L. Eggen, *Environ. Microbiol.*, 2001, **3**, 81-91
13 (DOI:10.1046/j.1462-2920.2001.00176.x).
14
15 23 J. Jacq, *J. Electroanal. Chem. Interfacial Electrochem.*, 1971, **29**, 149-180.
16
17 24 C. Batchelor-McAuley, Q. Li, S. M. Dapin and R. G. Compton, *J. Phys. Chem. B*, 2010, **114**, 4094-
18 4100 (DOI:10.1021/jp1008187).
19
20 25 C. E. Banks and R. G. Compton, *Anal. Sci.*, 2005, **21**, 1263-1268.
21
22 26 K. Kalcher, I. Svancara, R. Metelka, K. Vytras and A. Walcarius, *Encycl. Sens.*, 2006, **4**, 283-429.
23
24 27 V. Majer, J. Vesely and K. Stulik, *J. Electroanal. Chem. Interfacial Electrochem.*, 1973, **45**, 113-125
25 (DOI:10.1016/S0022-0728(73)80013-0).
26
27 28 G. G. Wildgoose, P. Abiman and R. G. Compton, *J. Mater. Chem.*, 2009, **19**, 4875-4886
28 (DOI:10.1039/b821027f).
29
30 29 R. L. McCreery, *Electroanalytical Chemistry*, 1991.
31
32 30 C. A. Thorogood, G. G. Wildgoose, J. H. Jones and R. G. Compton, *New J. Chem.*, 2007, **31**, 958-965
33 (DOI:10.1039/b700867h).
34
35 31 C. A. Thorogood, G. G. Wildgoose, A. Crossley, R. M. J. Jacobs, J. H. Jones and R. G. Compton,
36 *Chem. Mater.*, 2007, **19**, 4964-4974 (DOI:10.1021/cm071412a).
37
38 32 X. Ji, C. E. Banks, A. Crossley and R. G. Compton, *Chemphyschem*, 2006, **7**, 1337-1344.
39
40 33 *Pat.*, GB2490117, 1024; Patent Application Date: 20110418.; Priority Application Date: 20101104.
41
42 34 *Pat.*, WO2013009875, 0117; Patent Application Date: 20120711.; Priority Application Date:
43 20110712.
44
45 35 *Main IPC: G01N027-333. Pat.*, JP03243856, 1030; Patent Application Date: 19900222.; Priority
46 Application Date: 19900222.
47
48 36 *Main IPC: G01N027-30.; Secondary IPC: G01N027-48; C01B031-02. Pat.*, WO2005085825, 0915;
49 Patent Application Date: 20050304.; Priority Application Date: 20040304.
50
51 37 P. T. Lee, J. C. Harfield, A. Crossley, B. S. Pilgrim and R. G. Compton, *RSC Adv.*, 2013, **3**, 7347-7354
52 (DOI:10.1039/c3ra00164d).
53
54
55
56
57
58
59
60

1
2
3 38 A. T. Masheter, P. Abiman, G. G. Wildgoose, E. Wong, L. Xiao, N. V. Rees, R. Taylor, G. A. Attard, R.
4 Baron, A. Crossley, J. H. Jones and R. G. Compton, *J. Mater. Chem.*, 2007, **17**, 2616-2626
5 (DOI:10.1039/b702492d).
6

7 39 P. Abiman, G. G. Wildgoose, A. Crossley, J. H. Jones and R. G. Compton, *Chem. - Eur. J.*, 2007, **13**,
8 9663-9667 (DOI:10.1002/chem.200700942).
9

10 40 A. Savitzky and M. J. E. Golay, *Anal. Chem.*, 1964, **36**, 1627-1639 (DOI:10.1021/ac60214a047).
11

12 41 M. U. A. Bromba and H. Ziegler, *Anal. Chem.*, 1981, **53**, 1583-1586 (DOI:10.1021/ac00234a011).
13

14 42 Q. Li, C. Batchelor-McAuley, N. S. Lawrence, R. S. Hartshorne and R. G. Compton, *ChemPhysChem*,
15 2011, **12**, 1255-1257 (DOI:10.1002/cphc.201100174).
16
17

18 43 Q. Li, C. Batchelor-McAuley, N.S. Lawrence, R.S. Hartshorne, R.G. Compton, *Chem Comm*, 2011,
19 **47**, 11426.
20
21
22
23
24
25
26
27
28
29
30
31
32
33
34
35
36
37
38
39
40
41
42
43
44
45
46
47
48
49
50
51
52
53
54
55
56
57
58
59
60

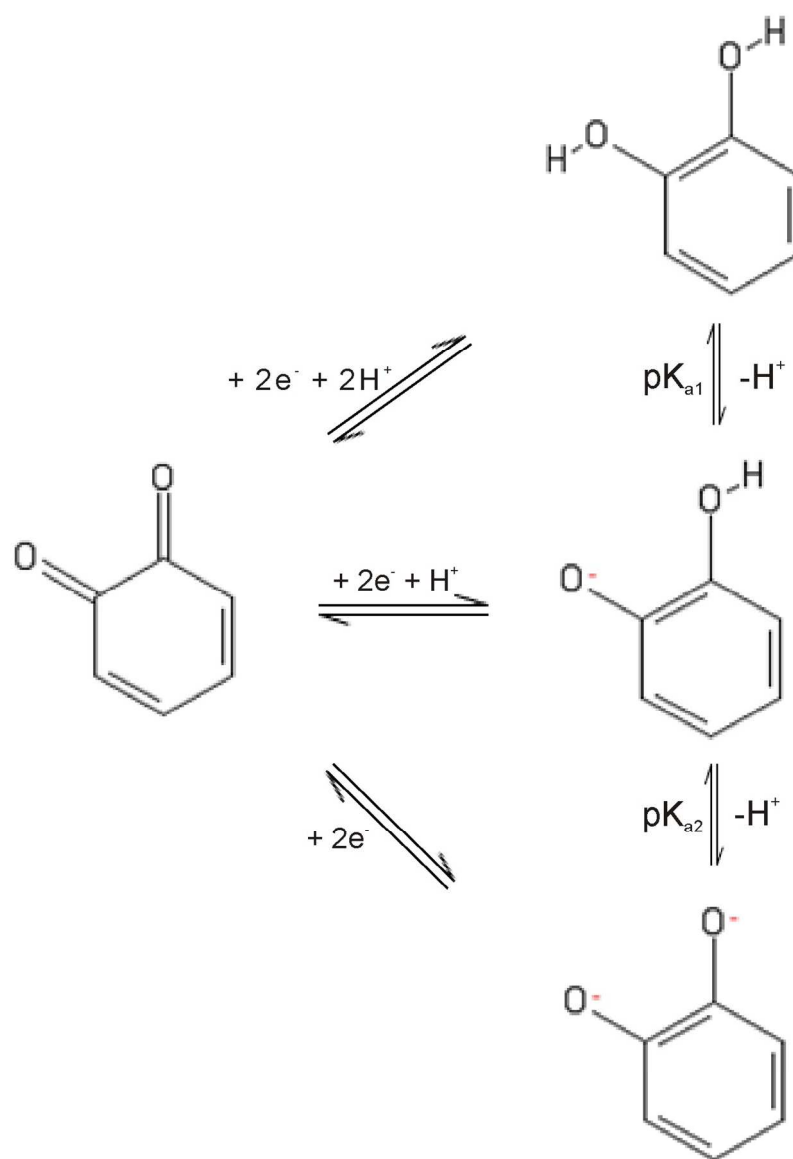


Fig 1. Schematic showing 3 pathways in which an orthoquinone molecule can be reduced in a $2e^-$ fashion with $m = 0, 1$ or 2
121x172mm (300 x 300 DPI)

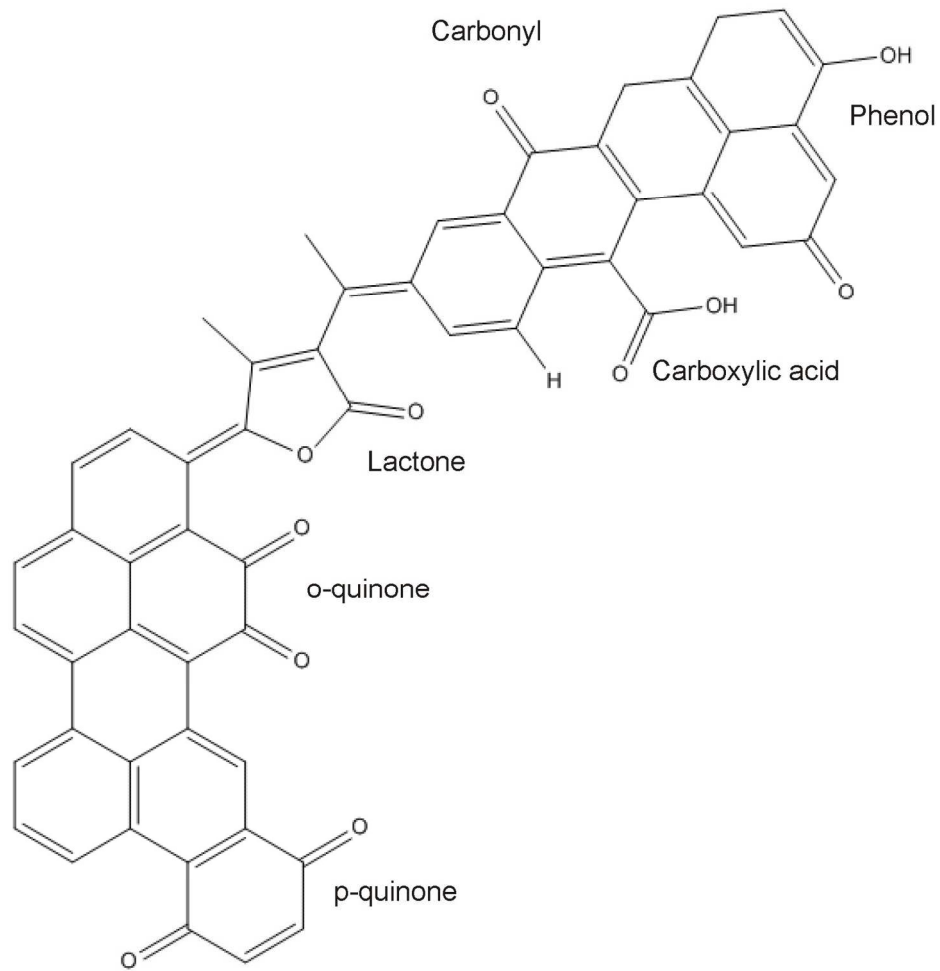


Fig 2. Representation of various functional groups present on graphitic carbon surfaces, adapted from reference [25]
152x148mm (300 x 300 DPI)

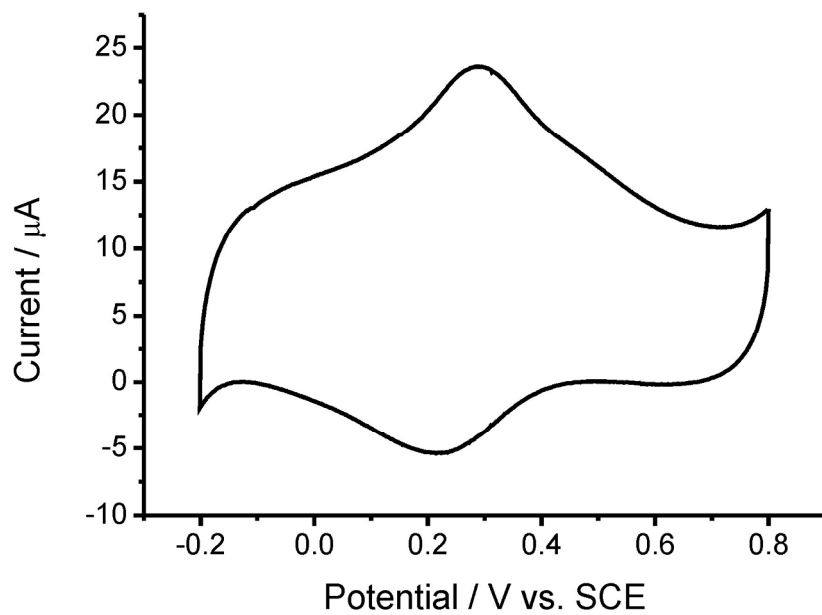


Fig 3. Typical CV of EPPG in 0.01 M HNO_3 + 100 mM KCl supporting electrolyte, from which surface coverage of quinone groups can be calculated
182x127mm (300 x 300 DPI)

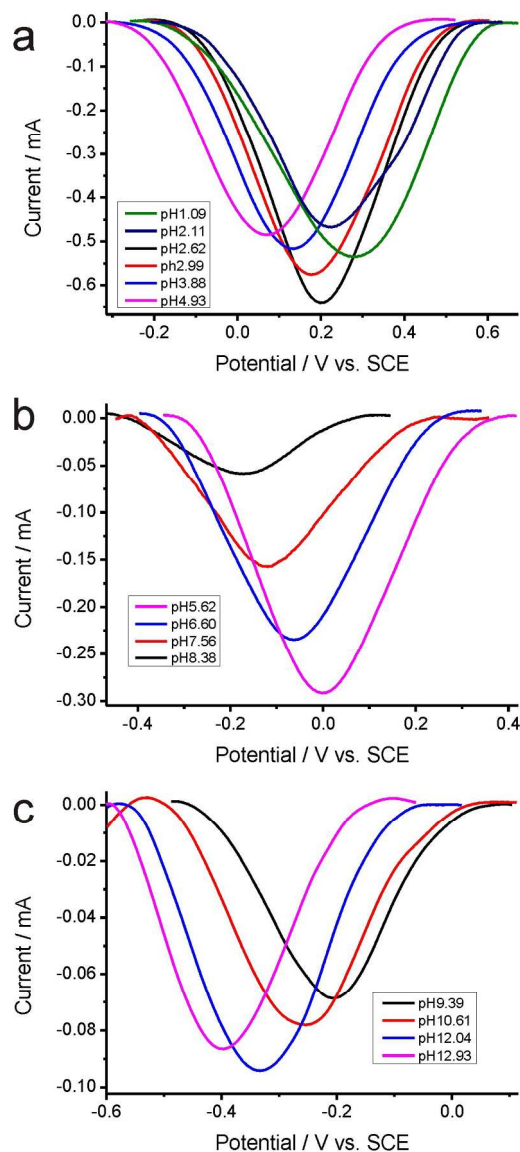


Fig 4. Quinone reduction peaks in square wave (SWV). 3 sets of peaks are shown, corresponding to the different media in which the reduction was performed; a) 0.01 M HCl/KCl buffer and citrate buffer (pHs: 2.11, 2.62, 2.99, 3.88, 4.93), 0.1 M HCl/KCl buffer at pH 1.09 b) 0.01M phosphate buffer (pHs: 5.62, 6.60, 7.56, 8.38), c) 0.01M carbonate buffer and NaOH solutions (pHs: 9.39, 10.61, 12.04, 12.93). SWV performed under optimised conditions: frequency – 150 Hz, step potential – 2 mV, amplitude – 200 mV 115x229mm (300 x 300 DPI)

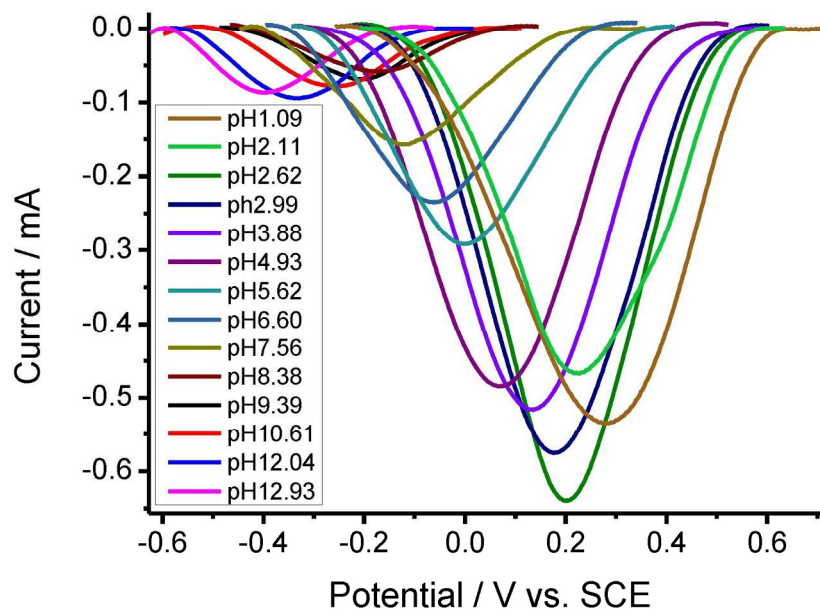


Fig 5. Quinone reduction peaks in square wave (SWV). Reduction peaks were obtained in different media (HCl/KCl buffer, citrate buffer, phosphate buffer, carbonate buffer and NaOH buffer solutions) at 0.01 M, ranging in pH from 2.11 to 12.93, 0.1 M HCl/KCl buffer at pH 1.09. SWV performed under optimised conditions: frequency – 150 Hz, step potential – 2 mV, amplitude – 200 mV
182x127mm (300 x 300 DPI)

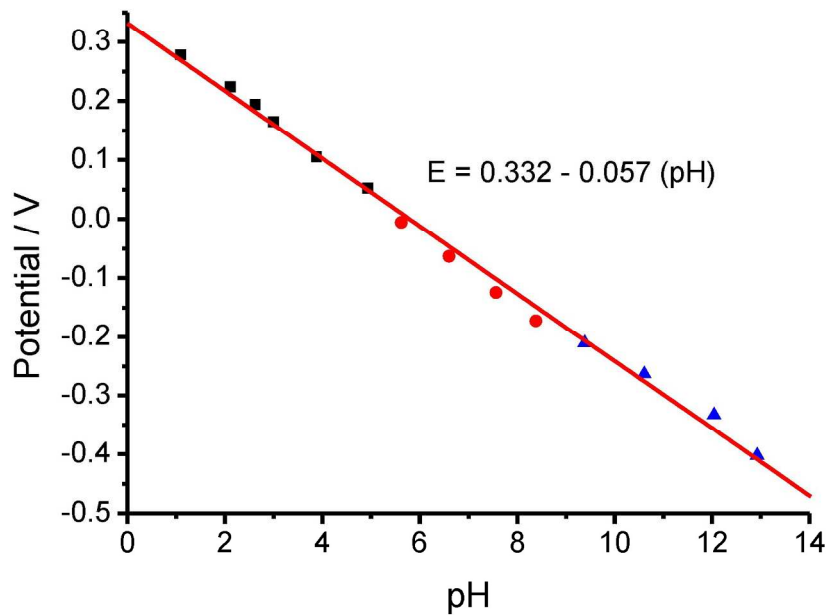


Fig 6. Calibration plot of SWV peak potential against pH for an EPPG in 0.01 M buffer solutions (with 0.1M HCl/KCl buffer solution at pH 1.09), showing a linear response with gradient of 57.0 mV / pH corresponding to a Nernstian behaviour. Black squares: low pH range, red circles: neutral pH range, blue squares: high pH range

182x127mm (300 x 300 DPI)

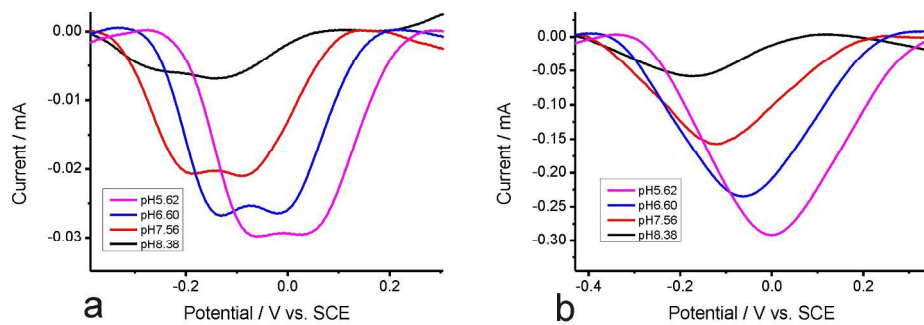


Figure 7. Reduction peaks on EPPG electrode in 0.01 M phosphate buffer solution, 7a) shows reduction peaks with amplitude 20 mV, whereas 7b) shows the peak under optimised conditions of amplitude 200 mV
223x80mm (300 x 300 DPI)

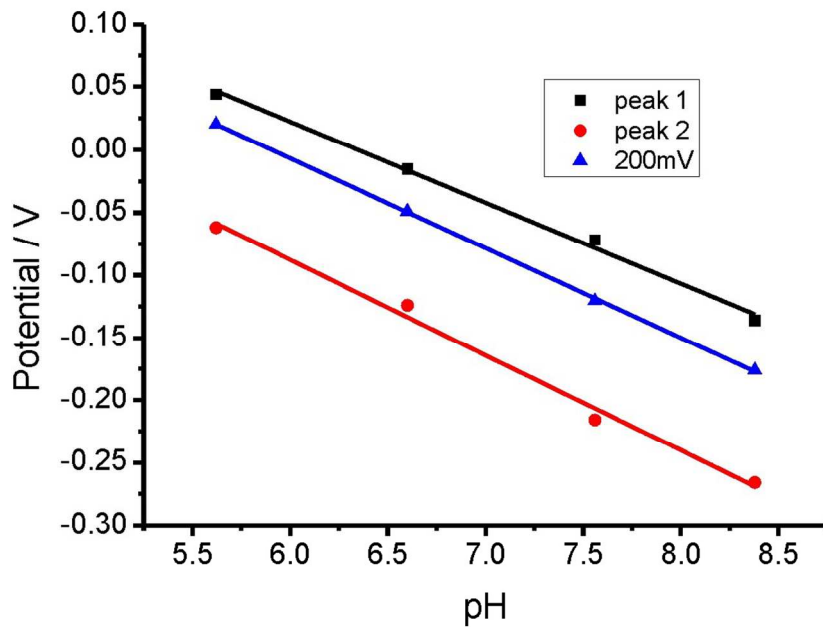


Figure 8. Calibration plot showing both peak 1 and peak 2 of the double peak reduction in 0.01 M phosphate buffer with amplitude 20 mV. Calibration for the reductions performed at 200 mV are shown as blue triangles, intermediate of the 2 peaks at 20 mV amplitude
115x80mm (300 x 300 DPI)

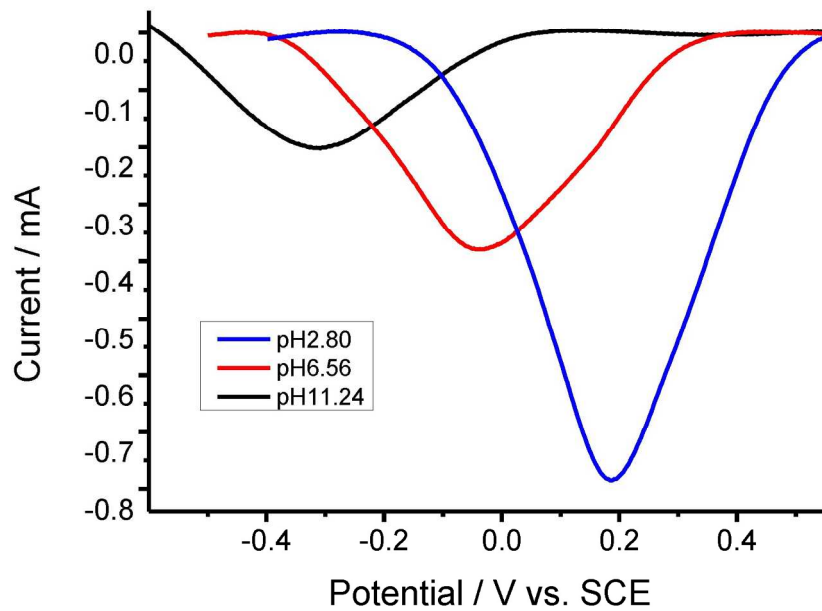


Figure 9. Reduction peaks of EPPG in 0.1 M buffer solutions (pH 2.80 citrate buffer solution, pH 6.56 phosphate buffer solution, pH 11.24 carbonate buffer solution)
182x127mm (300 x 300 DPI)

1
2
3
4
5
6
7
8
9
10
11
12
13
14
15
16
17
18
19
20
21
22
23
24
25
26
27
28
29
30
31
32
33
34
35
36
37
38
39
40
41
42
43
44
45
46
47
48
49
50
51
52
53
54
55
56
57
58
59
60

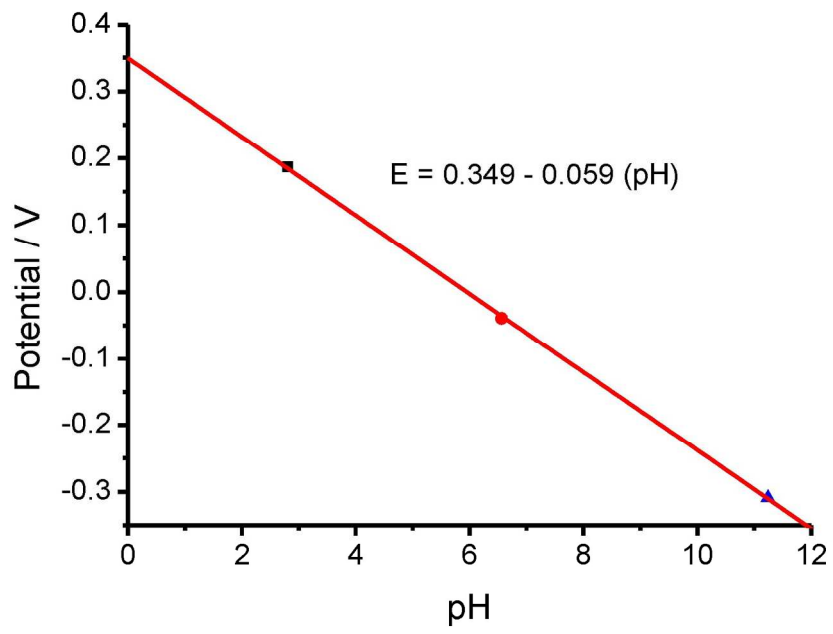


Figure 10. Calibration plot of the reduction peaks in 0.1 M buffer solutions. Back square corresponds to citrate buffer, red circle corresponds to phosphate buffer and blue triangle corresponds to carbonate buffer
170x119mm (300 x 300 DPI)

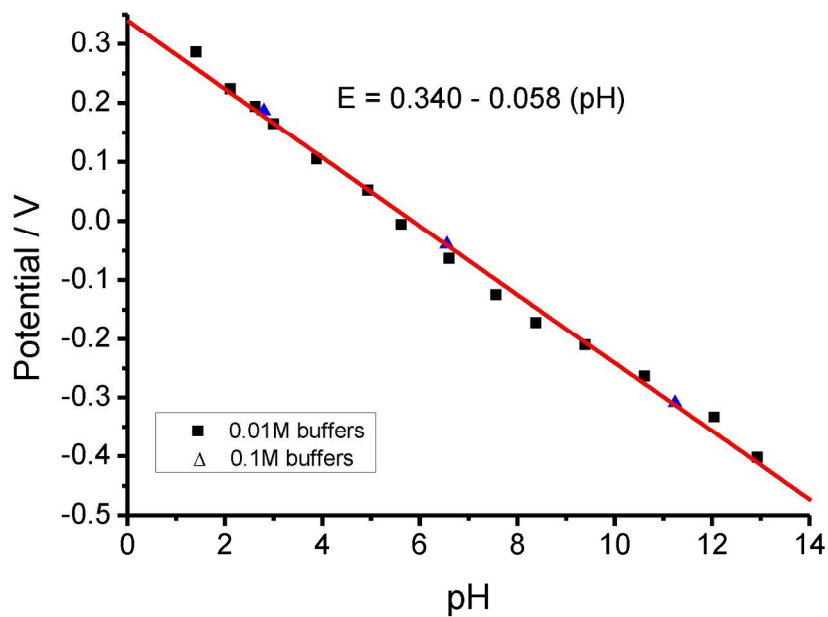


Figure 11. Calibration plot of the original reduction points in 0.01 M buffer solutions (black triangles), with reduction points of 0.1 M buffer solutions (blue triangles) added for comparison
182x127mm (300 x 300 DPI)